Ultrafast Conformational Dynamics in Cyclic Azobenzene Peptides of Increased Flexibility

J. Wachtveitl,* S. Spörlein,† H. Satzger,† B. Fonrobert,† C. Renner,‡ R. Behrendt,‡ D. Oesterhelt,‡ L. Moroder,‡ and W. Zinth†

*Institut für Physikalische und Theoretische Chemie, Goethe-Universität Frankfurt, 60439 Frankfurt, Germany; †Sektion Physik, Ludwig-Maximilians-Universität München, 80538 Munich, Germany; and ‡Max-Planck-Institut für Biochemie, 82152 Martinsried, Germany

ABSTRACT Structural changes of peptides containing the azobenzene dye 4-aminomethyl-phenylazobenzoic acid (AMPB) are studied with ultrafast spectroscopy. AMPB peptides are a new class of molecules where the photoisomerizable dye azobenzene is linked to the peptide moiety via a flexible methylene spacer. The ultrafast reactions in the femtosecond to nanosecond time domain are investigated for the optical switch AMPB, a linear and cyclic octapeptide, and a bicyclic octapeptide containing an additional disulfide bridge. These molecules with increasing conformational constraints are studied for the *cis* to *trans* and the *trans* to *cis* photoreactions. For the *cis* to *trans* reaction the isomerization of the chromophore occurs fast in the 1-ps range, whereas it is slower (10-ps range) in the *trans* to *cis* reaction. In all peptides the structural changes of the chromophore lead to modifications in the peptide structure in the 10-ps–1-ns time range. The results indicate that the chromophore AMPB acts simultaneously as a fast molecular switch and as a sensor for initial conformational dynamics in the peptide. Experiments in the mid-infrared range where the structural changes of the peptide backbone are directly observed demonstrate that the essential part of the structural dynamics in the bicyclic AMPB peptide occurs faster than 10 ns.

INTRODUCTION

During the process of protein folding a linear chain of amino acids adopts helical and sheet-like structures in a series of complex reaction steps finally leading to the three-dimensional arrangement of the functional active, native protein. The timescale of the protein folding process usually covers several orders of magnitude, extending from microseconds to the range of several hours (Frauenfelder et al., 1991; Dill and Chan, 1997). For a more profound understanding of the mechanisms and determinants of this complex process, a synchronized reaction initiation and a subsequent observation with sufficient time resolution is required. Experimentally, the elementary events of protein folding have been addressed by stopped flow experiments in the millisecond timescale (Pollack et al., 2001). Laser induced pH and temperature jump experiments as well as triplet-triplet energy transfer experiments opened up the nanosecond range and showed that basic structural elements are formed on this timescale (Ballew et al., 1996; Williams et al., 1996; Gilmanshin et al., 1997; Munoz et al., 1997; Duan and Kollman, 1998; Bieri and Kiefhaber, 1999; Bieri et al., 1999; Daura et al., 1999; Zhou and Karplus, 1999; Thompson et al., 2000; Huang et al., 2002a,b; Werner et al., 2002). An even higher time resolution could be achieved with a molecular switch incorporated in the peptide chain. Fast conformational dynamics was observed after photoinduced disulfide cleavage (Volk et al., 1997). Recently, a new technique was introduced that allowed reversible photocontrol of the conformation of a cyclic peptide (Spörlein et al., 2002; Bredenbeck et al., 2003). In these experiments an azobenzene unit was incorporated directly into the backbone of a cyclic peptide. This guarantees that the light-induced structural changes of the chromophore upon photoisomerization around the central N=N double bond are directly transferred to the peptide chain (Behrendt et al., 1999a; Renner et al., 2000a,b). On the other hand, it was shown for a related azopeptide that the conformational dynamics of the peptide chain influences the visible chromophore absorption. In these experiments, transient processes were found on the 50-ps timescale and could be assigned to conformational dynamics of the peptide part (Spörlein et al., 2002).

In this article, we present investigations on the next generation of model peptides that extends the versatility of the earlier approach where 4-amino-phenylazobenzoic acid (APB) was employed as optical switch.

1. A modified chromophore 4-aminomethyl-phenylazobenzoic acid (AMPB) is used as a trigger molecule (Fig. 1). The introduction of a CH_2 spacer between the phenyl ring and the amino group adds a new element of flexibility. Due to its increased geometric length, AMPB can serve as dipeptide mimic within the peptide (Ulysse and Chmielewski, 1994; Ulysse et al., 1995; Renner et al., 2000b). The peptide of choice was the active site octapeptide fragment of thioredoxin reductase (H-Ala-Cys-Ala-Thr-Cys-Asp-Gly-Phe-OH), with the ultimate scope of photomodulating the redox properties of this bis-cysteinyl-peptide as mimic of thiol/disulfide oxidoreductases.
2. In a comparative study, different AMPB molecules are analyzed. The free chromophore AMPB, the linear peptide construct (l-AMPB), the monocyclic (c-AMPB), and the bicyclic compound (bc-AMPB) are analyzed

Submitted July 11, 2003, and accepted for publication November 26, 2003.

Address reprint requests to J. Wachtveitl, E-mail: wveitl@theochem.uni-frankfurt.de.

0006-3495/04/04/2350/13 $2.00

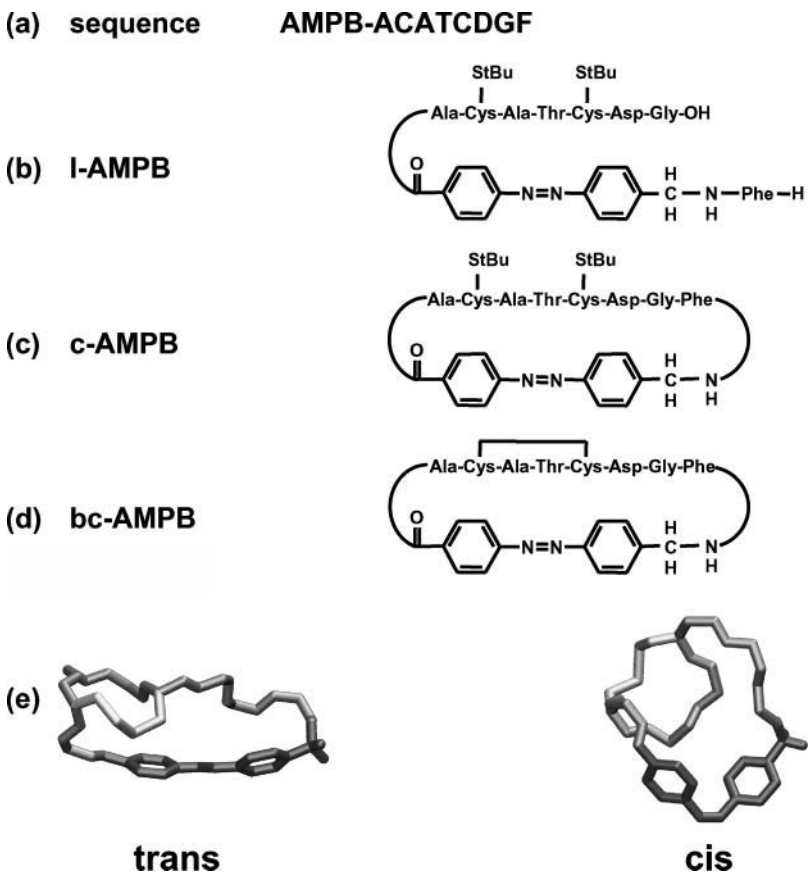

FIGURE 1 Sequence (*a*) and schematic sketch of linear (*b*), monocyclic (*c*), and disulfide-bridged bicyclic AMBP peptides (*d*). Reversible photomodulation of conformation of the bicyclic AMBP peptide according to the NMR structures (*e*) given in (Renner et al., 2000b). The *trans* → *cis* photoisomerization of the AMPB photoswitch (*dark gray*) allows the formation of a distorted helix-like structure from the initial elongated molecular conformation. The peptide backbone is shown in gray and the Cys–Cys bond in light gray.

(Fig. 1). The disulfide bridge between the two cysteine residues in bc-AMPB strongly reduces the accessible conformational space of the peptide. This leads to a well-defined conformation for the *trans* azoisomer and a significant light-induced conformational transition of the peptide moiety upon isomerization (Renner et al., 2000b). In the linear precursor molecule l-AMPB, the peptide chain is opened between the glycine and the phenylalanine residue. The photoresponsive properties are conserved for an analogous water-soluble cyclic bis-cysteinyl-peptide (Renner et al., 2002). Recently, a photomodulation of its bioactivity, i.e., its efficiency as oxidative refolding agent, could be demonstrated for this system (Cattani-Scholz et al., 2001).

3. To address the dynamic consequences for a reaction, where the accessible conformational space for the respective cyclopeptide is restricted or enlarged, both directions of the isomerization reaction (i.e., the *cis* → *trans* and the *trans* → *cis* direction) were studied.

EXPERIMENTAL METHODS

Sample preparation

The syntheses of 4-aminomethyl-phenylazobenzoic acid as well as of the linear, monocyclic, and bicyclic AMPB peptides were reported elsewhere (Behrendt et al., 1999b). All samples were dissolved in dimethylsulfoxide (DMSO) to ensure a good solubility and to allow spectroscopic experiments both in the visible (vis) and the mid-infrared (MIR) spectral region. The results could then be compared directly to the NMR structural analyses, which were also carried out in DMSO as solvent (Renner et al., 2000b). Due to the different absorption properties of the *cis* and *trans* isomers, the concentrations in the time-resolved experiments had to be adjusted accordingly; typical concentrations were between 0.5 mM (*cis*) and 3.5 mM (*trans*). Both the molecular switch AMPB and the AMPB peptides are bistable, i.e., the isomer ratio can be changed by illumination. Therefore the photoexcited sample volume had to be exchanged between the individual laser pulses. For the femtosecond experiments, this was achieved by pumping the solution with a sufficient flow rate through the fused silica flow cuvette (0.5-mm optical pathlength). In the nanosecond-IR experiments, the CaF_2 cuvette was mounted on a rotation/translation stage and displaced with sufficient velocity.

The initial *cis*-isomeric state was prepared by continuous-wave (cw) illumination with light between 320 nm and 380 nm (1-kW high pressure HgXe arc lamp with UG11 and WG320 filters, Fa. Schott, Mainz, Germany) supplied via a liquid-light guide. For the preparation of the *trans* isomer, the sample was irradiated around 450 nm using a combination of GG 435 and BG 12 filters. The UV/visible spectra of both isomers were recorded on a Lambda 19 spectrometer (Perkin Elmer, Wellesley, MA). In the photostationary state reached after illumination, ~85% of the molecules were in the *cis* form.

Time-resolved spectroscopy

The visible pump/white-light probe setup for femtosecond time-resolved transient absorbance measurements was reported in detail elsewhere (Huber

et al., 2001; Spörlein et al., 2002). In brief, the laser source is a home-built Ti-sapphire regenerative amplifier system with 1-mJ pulse energy at 800 nm and 1-kHz repetition rate at a pulse duration of 100 fs (full width at half-maximum). Tunable pump pulses are generated by frequency doubling the 800-nm output in a BBO crystal. The resulting 400-nm light is converted in a two-stage noncollinear optical parametric amplifier (NOPA) to produce excitation pulses at $\lambda_{exc} = 480$ nm (Wilhelm et al., 1997; Huber et al., 2001). After compression, the output pulses of the noncollinear optical parametric amplifier have a typical pulse duration between 40 fs and 80 fs. The white-light continuum used for probing is generated in CaF_2. This modification resulted in a drastically increased probing range; spectra from 320 nm to 650 nm could be recorded simultaneously (Huber et al., 2001). However, CaF_2 is more sensitive to photodestruction than the commonly used sapphire and had to be continuously displaced during the experiment. For the detection, two separate spectrometers are used each with a 42-segment diode array ($\Delta\lambda = 8$ nm) as described in Seel et al. (1997). The time resolution of the experiment was determined by the cross-correlation function between the pump and the white-light probe pulse having a typical width between 50 fs and 90 fs. The processing of the measured transient absorption data includes correction for dispersion and solvent effects, normalization, and calculation of the response of the pure initial states (Huber et al., 2002; Spörlein et al., 2002). A global fitting procedure was used to determine the kinetic constants of the reactions under the assumption of a rate equation system.

IR spectroscopy

The FTIR spectra were recorded on a Bruker IFS66 spectrophotometer (Bruker, Ettlingen, Germany) equipped with a deuterated tryglycine sulphate (DGTS) detector (resolution ≈ 2 cm^{-1}) with an illumination device for the preparation of both *cis* and *trans* isomers as described above. The sample temperature was kept constant within ± 0.5°C. Samples were dissolved in DMSO-d_6 (concentrations 10 mM) and placed in a home-built IR cuvette (CaF_2 windows, 100-μm or 50-μm optical pathlength).

The nanosecond time-resolved transient absorption measurements were performed with a home-built nanosecond-UV pump/cw-IR probe setup. Light in the MIR spectral region emitted from a double-heterostructure diode-laser (Mütek, Diessen, Germany; Laser Components, Olching, Germany) is imaged via planar and off-axis parabolic gold-coated mirrors through the sample onto a fast mercury-cadmium-telluride (MCT) detector with an active area of (0.25×0.25) mm^2 (Kolmar, Newburyport, MA). The effective rise time is below 10 ns. The frequency of the probe light could be varied between 1500 cm^{-1} and 1700 cm^{-1} and gives access to the different vibrational responses in this spectral range. The excitation pulses at 355 nm (pulse energy 35 μJ) are generated by a Q-switched, frequency-tripled Nd:YAG laser (Continuum, Santa Clara, CA) at a repetition rate of 2 Hz. The UV light for excitation was transferred to the sample by a 250-μm multimode fiber and a $f = 50$-mm quartz lens. The spot diameters within the cuvette were 210 μm (IR probe) and 700 μm (UV pump), respectively. For a given sample thickness (50 μm) and concentration (10 mM) this allows an absolute scaling of the signal heights and a comparison to the cw-FTIR spectra. To avoid accumulation of photoproducts, the sample is exchanged after each pulse. Steady-state illumination maintained a constant isomer ratio with high *trans* concentration for the subsequent measurements. After detection and amplification, the transient data recorded with and without excitation are recorded in a digital oscilloscope (Tektronix, Beaverton, OR; type TDS 5054). In total, 3000–10,000 single traces were averaged and subsequently converted into scaled transient absorption changes. To allow a visualization of the transient absorption changes from a few nanoseconds to milliseconds (Fig. 3 *b*), the data are plotted on a combined linear-logarithmic timescale. Due to electronic noise from the Q-switched Nd:YAG laser and density fluctuations in the sample, induced by the pumping pulses, the recorded signal traces exhibit strong oscillations between 10 ns and 5 μs.

EXPERIMENTAL RESULTS

Spectroscopic properties of the samples

In this study, AMPB is employed as optical switch. Upon *cis* → *trans* isomerization, the distance between the nitrogen at the amino end and the carbon at the carboxyl end of AMPB changes from 7 Å to 12 Å. The absorption spectrum of AMPB (Fig. 2) shows the basic features known from azobenzene (Rau, 1990). The $\pi\pi^*$ band of AMPB is red shifted to 343 nm as compared to free azobenzene ($\lambda_{max} = 320$ nm). This is due to the polar character of the amino and the carboxyl group (Table 1). As compared to APB, where the peak is shifted to 420 nm, the presence of the CH_2 group in AMPB disrupts the conjugated π-system and therefore significantly reduces the red shift. As a consequence, the $n\pi^*$ absorption at 450 nm (which extends out to 500 nm) is observed as a separate band. In the *cis* form, the $n\pi^*$ absorption is slightly increased. The dominant feature of the *cis* spectrum is the appearance of the $\pi\pi^*$ band at 260 nm and the strong decrease of the corresponding *trans* $\pi\pi^*$ band at 343 nm.

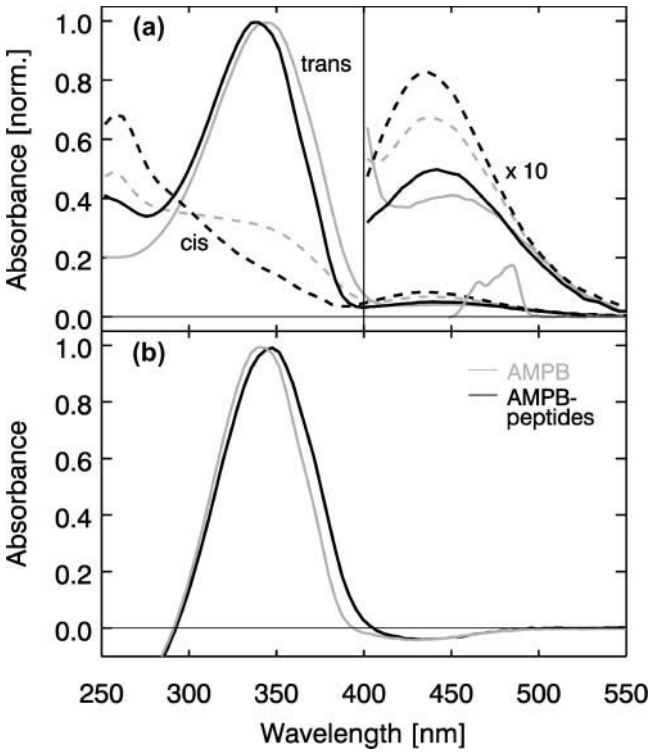

FIGURE 2 (*Top*) Absorption spectrum of the *trans* (*solid lines*) and *cis* isomers (*dashed line*) of AMPB (*gray*) and c-AMPB peptide in DMSO. The maxima of the *trans* $\pi\pi^*$ bands are scaled to 1; the absorption scale for $\lambda >$ 400 nm is enlarged by a factor of 10 for a better visibility of the $n\pi^*$ bands. The spectrum of the excitation pulse used in the femtosecond experiments is tuned to the long wavelength side of the $n\pi^*$ band. (*Bottom*) *trans*-minus-*cis* difference spectra for AMPB (*gray*) and AMPB peptides. The spectra for the different peptides are very similar.

TABLE 1 Absorption properties of azobenzene, AMPB, and AMPB peptides in DMSO

	λ_{max} (nm)				
	trans		*cis*		
Sample	$\pi\pi^*$ band	$n\pi^*$ band	$\pi\pi^*$ band	$n\pi^*$ band	*trans* content in photostationary state
Azobenzene	322	445	288	432	≤10%
AMPB	343	450	257	437	≤20%
l-AMPB	339	444	257	434	≤10%
c-AMPB	338	445	258	435	≤10%
bc-AMPB	338	445	256	430	≤10%

Addition of the different peptide parts affects the absorption properties of the AMPB chromophore in a very similar fashion (Table 1 and Fig. 2 *a*). As compared to free AMPB, the maximum of the *trans* $\pi\pi^*$ band is only slightly shifted to the blue ($\lambda_{max} = 339$ nm). Also the photoselective properties of the optical switch are retained in the linear and (bi)cyclic AMPB peptides: the photoisomerization both in the *cis* → *trans* and the *trans* → *cis* direction of the AMPB moiety can be induced via $n\pi^*$ excitation. The photoreaction proceeds with high quantum yield and leads to spectrally clearly distinguishable isomers. The *cis* configuration is metastable. At room temperature it reacts back to the stable *trans* form on the timescale of hours (Renner et al., 2000b). The absorption spectra of the different samples are very similar. Therefore only the spectra for both isomers of one peptide (c-AMPB) are shown in Fig. 2 *a*. The difference spectra of all three AMPB peptides upon isomerization (the *cis* → *trans* direction is shown in Fig. 2 *b*) are virtually indistinguishable: all AMPB peptides exhibit the extrema of their absorption changes around 435 nm ($n\pi^*$ band) and 340 nm ($\pi\pi^*$ band) and reveal an isosbestic point at 290 nm. Although the steady-state visible spectra reflect predominantly the chromophore part of the molecule, the IR spectra (Fig. 3 *a*) monitor both the chromophore and the peptide part. In the free chromophore AMPB, the photoisomerization induces absorption changes at frequencies below 1625 cm^{-1} (Fig. 3 *a*, *top*). For the cyclic (data not shown) and bicyclic AMPB peptides (Fig. 3 *a*, *bottom*), strong absorption changes occur at higher frequencies between 1625 cm^{-1} and 1725 cm^{-1}. They can be attributed to changes of the amide I band caused by the peptide part of the molecule. The amide I band originates mainly from C=O stretch motions and is known to reflect structural changes of the peptide backbone (Krimm and Bandekar, 1986; Torii and Tasumi, 1992, 1998). The weak absorption changes found below 1630 cm^{-1} should be connected with both structural changes of the chromophore and the peptide (amide II band). For the

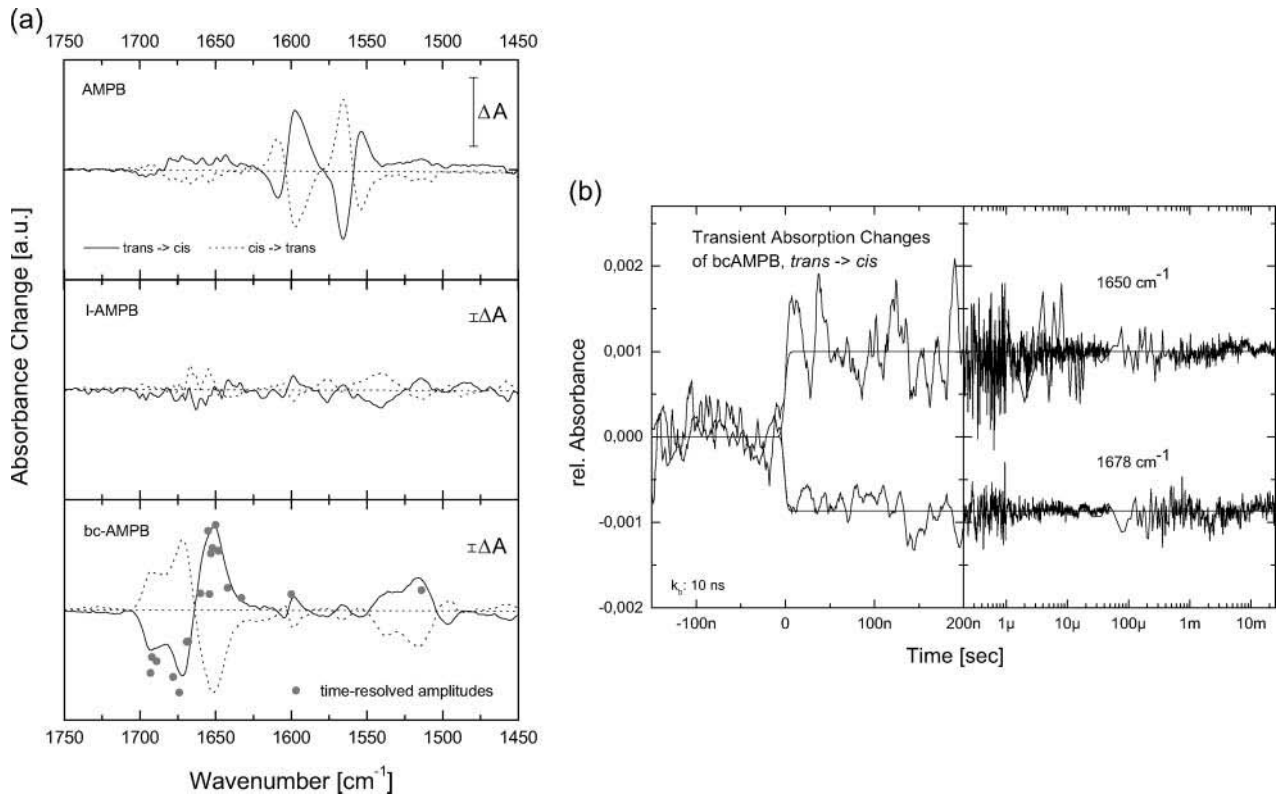

FIGURE 3 (*a*) Steady-state difference spectra for AMPB and the corresponding linear and bicyclic AMPB peptides for both isomerization directions in the mid-IR spectral region. (*b*) Transient absorbance changes of the bicyclic AMPB peptide at two different frequencies in the amide I band. The signal amplitude of the transients observed at 10 ns at various frequencies is plotted in *a* (*bottom, shaded dots*).

linear AMPB peptide, only weak absorption changes are present in the amide I range. This gives the first indication that only minor persistent conformational changes of the peptide part are induced in l-AMPB upon photoisomerization of the AMPB chromophore.

Time-resolved absorption changes

For a direct analysis of the backbone dynamics in response to the AMPB photoisomerization, transient vibrational spectroscopy of the amide I and amide II bands with 10-ns time resolution is applied. Before the 355-nm excitation pulse, the sample was predominantly in the *trans* form. Thus the observed absorption changes result from the *trans* to *cis* reaction. Two selected transients for bc-AMPB recorded at the frequencies 1650 cm^{-1} and 1678 cm^{-1}, both in the amide I band, are shown in Fig. 3 *b*. These and further experiments at 15 different spectral positions (including one in the amide II band at 1520 cm^{-1}) demonstrate that the major absorption changes occur within the instrumental response time, i.e., faster than 10 ns. From 10 ns to 10 ms, no distinct changes in the signal amplitudes are observed. However, sign and amplitude of the signals vary with frequency. A comparison of these signal amplitudes with the cw *trans*-minus-*cis* difference spectrum (Fig. 3 *a*, *bottom*) shows a similar spectral dependence of the two experiments. These findings indicate that the main conformational changes of the peptide backbone are completed after a few nanoseconds. The faster conformational transitions of the peptide backbone upon *cis* to *trans* photoisomerization were recently analyzed by picosecond-IR spectroscopy and are reported elsewhere (Bredenbeck et al., 2003).

In Fig. 4, examples for ultrafast transient absorption data of the monocyclic c-AMPB peptide after excitation with pulses in the $n\pi^*$ band at 480 nm are presented. The sample was initially in the *cis* (*a*) or *trans* (*b*) state, respectively. The absorption changes are plotted as a function of time delay t_D (on a logarithmic scale) and probing wavelength λ_{pr} (on a linear scale) and represent the *cis* → *trans* (*a*) and the *trans* → *cis* (*b*) reaction. The data are displayed for delay times $t_D > 20$ fs (Fig. 4 *a*) and 100 fs (Fig. 4 *b*), respectively, i.e., for times where the fast initial transients around time 0 related with the excitation process have decayed. Transient absorption changes occur throughout the whole investigated range until 1 ns. For a qualitative discussion of the light-induced reaction we will focus at first on characteristic wavelength ranges. For this purpose, Fig. 5 illustrates the transient difference absorption spectra for the various samples recorded at specific times after the excitation pulse (*highlighted* in Fig. 4), together with the stationary difference spectra. The transient difference spectra are plotted in Fig. 5 for delay times of 0.2 ps, 2 ps, and 20 ps and for the cw experiment for both the *cis* → *trans* (Fig. 5, *a*, *c*, *e*, and *g*) and the *trans* → *cis* (Fig. 5, *b*, *d*, *f*, and *h*) reaction.

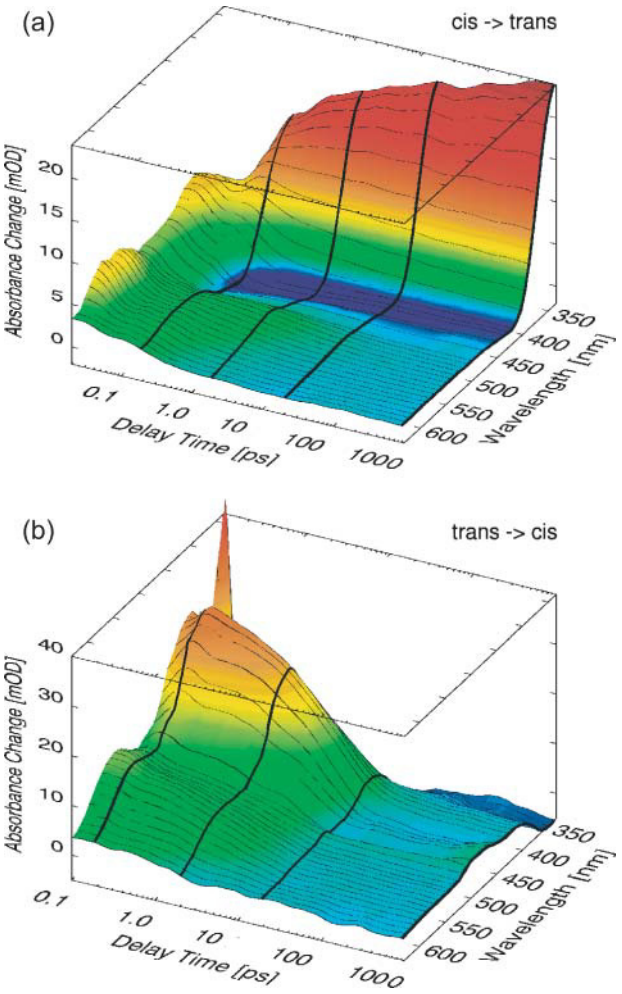

FIGURE 4 Transient absorption changes of c-AMPB for the *cis* → *trans* (*top*) and the *trans* → *cis* (*bottom*) reaction for different delay times and probing wavelengths. The white-light probe pulses covered a spectral range from 350 nm to 650 nm; the thick lines along selected delay times (200 fs, 2 ps, 20 ps, and 1 ns) represent the individual transient spectra depicted in Fig. 5, *e* and *f*.

General spectral characteristics

At very long probe wavelengths ($\lambda_{pr} > 560$ nm) for the *cis* → *trans* (*left side* of Fig. 5) reaction, an early absorption increase is observed that decays rapidly on the subpicosecond (~200 fs) and picosecond (~1.3 ps) timescale. This process can be assigned to excited state absorption and its decay upon internal conversion. At shorter probe wavelengths (480–550 nm), the decay of the induced absorption is somewhat slower, with a dominant kinetic component in the 10-ps range. Subsequently, weak absorption changes occur on the 100-ps range in the case of the AMPB peptides. The absorption in this region exhibits a spectral blue shift (e.g., for bc-AMPB $\lambda_{max} = 570$ nm for $t_D = 0.2$ ps, $\lambda_{max} = 530$ nm for $t_D = 2$ ps, and $\lambda_{max} = 510$ nm for $t_D = 200$ ps). In c-APB such a shift was related to cooling of the vibrationally hot chromophore at early times and the subsequent relaxation of

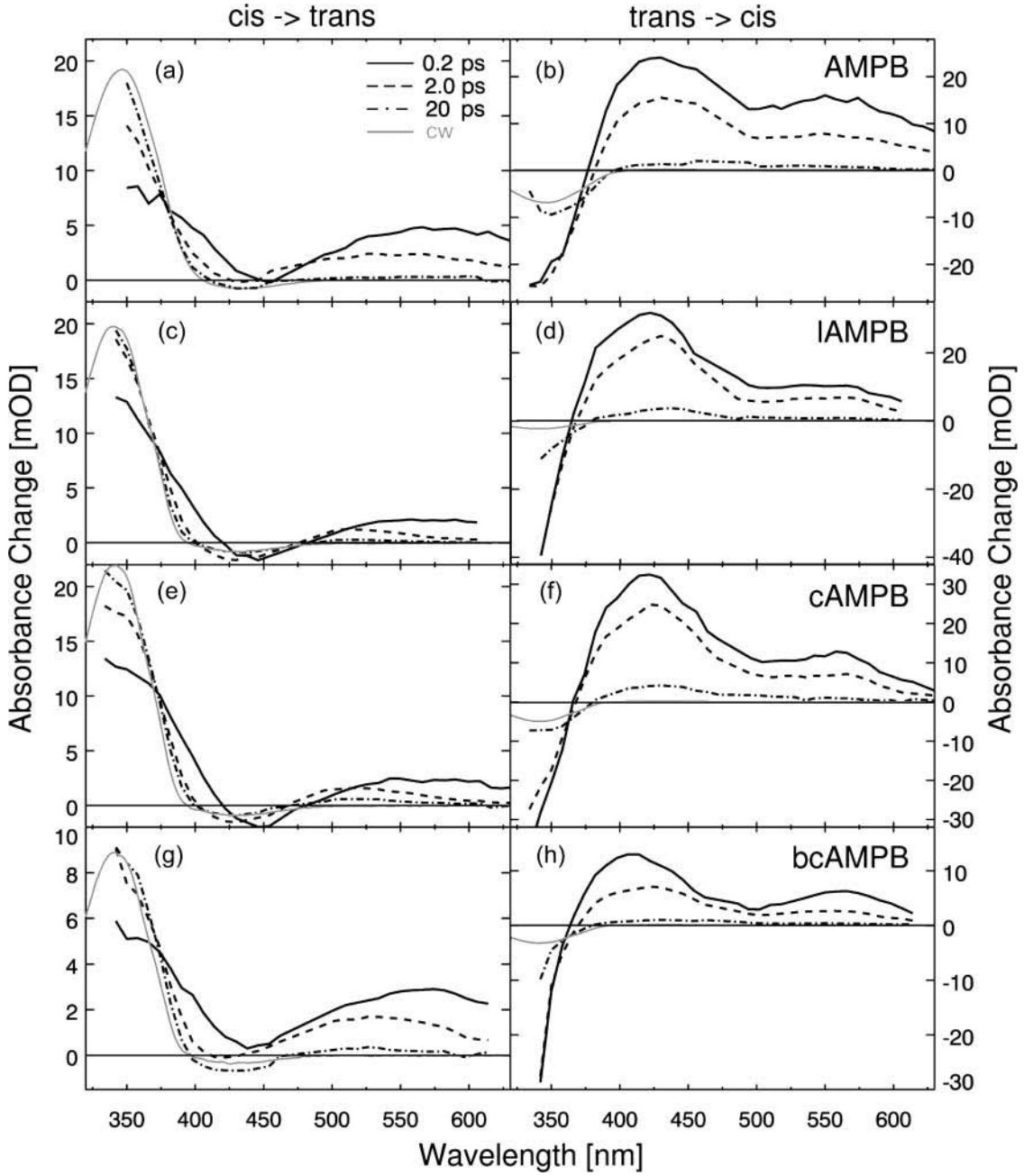

FIGURE 5 Transient spectra for AMPB (*a* and *b*) and the corresponding linear (*c* and *d*), cyclic (*e* and *f*), and bicyclic peptides (*g* and *h*) for delay times of 200 fs, 2 ps, and 20 ps together with the respective steady-state difference spectra.

strain between chromophore and peptide (Spörlein et al., 2002).

At probe wavelengths shorter than the excitation wavelength, the dominant spectral features after the decay of the excited state are the bleaching of the $n\pi^*$ band (around 430 nm) of the *cis* isomer and the formation of the strong $\pi\pi^*$ transition of the *trans* form of the chromophore (below 400 nm). In this spectral range a delayed rise of the absorption and spectral shifts ($\leq$10 nm in the 50-ps time range) can be observed.

For the *trans* $\rightarrow$ *cis* isomerization (Fig. 4 *b*), the absorption transients differ considerably from those of the *cis* to *trans* reaction. Most obvious are the disappearance of the *trans* $\pi\pi^*$ band in the blue part of the spectrum and the decay of the excited state absorption on the 2–10-ps timescale. At later delay times there are weak absorption changes on the 100-ps timescale, and the system finally reaches an absorption spectrum, which closely resembles the spectral changes found in the cw experiment.

Detailed analysis and modeling of the transient absorption changes

More quantitative conclusions on the molecular processes occurring at different delay times can be obtained from the inspection of the transient absorption spectra (change in absorption recorded at certain delay times; see Fig. 5) and from the results of the global fitting procedure. The decay associated spectra related with the different time constants are shown in Fig. 6. In the global fitting procedure, different numbers of time constants were used. The best consistent fit was obtained using four or five kinetic components for each sample (see Table 2; the same time constants are used for all probe wavelengths of one sample and one direction of the photoreaction). We are aware of the fact that exponential kinetics are well suited to describe reactions between well-defined thermally relaxed intermediate states. Since the investigated conformational dynamics may start from a distribution of conformations, proceed via different pathways, and end in a distribution of conformations, the use of exponential modeling can only be taken as a first order approximation. In this context, it should be noted that the

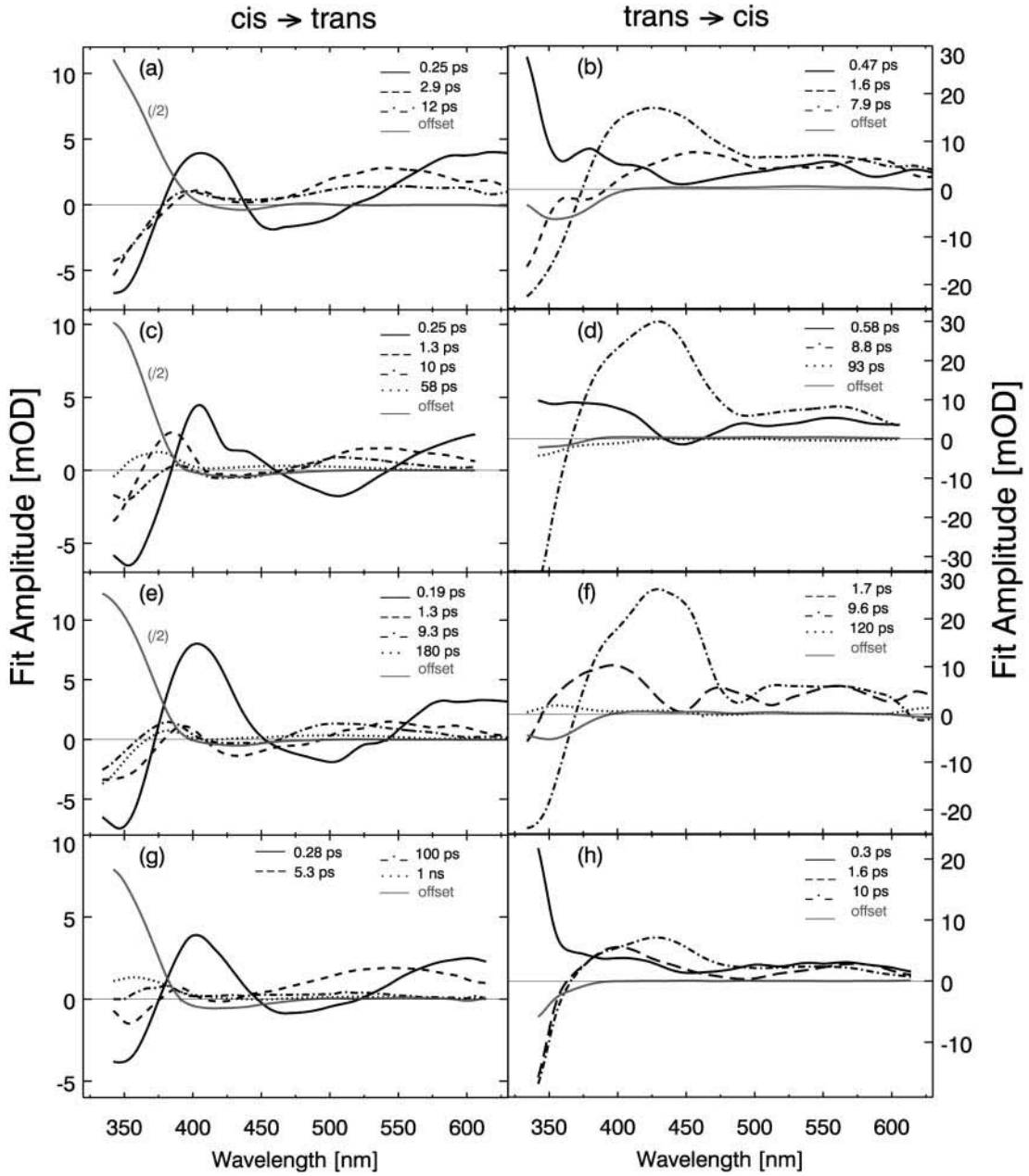

FIGURE 6 Amplitude spectra for AMPB (*a* and *b*) and the corresponding linear (*c* and *d*), cyclic (*e* and *f*), and bicyclic peptides (*g* and *h*) derived from a global fitting routine.

TABLE 2 Time constants derived from the global fitting routine for the transient absorbance changes of AMPB and AMPB peptides for both isomerization directions

Sample	Time constants (ps)							
	trans → *cis*				*cis* → *trans*			
AMPB	0.47	1.6	7.9		0.25	2.9	12	
l-AMPB	0.58		8.8	93	0.25	1.3	10	58
c-AMPB		1.7	9.6	120	0.19	1.3	9.3	180
bc-AMPB	0.3	1.6	10		0.28	5.4		100; 1000

The time constants with similar amplitude spectra (see Fig. 6) are placed in the same column. The time constants result from multiexponential modeling of the observed absorption transients. Usually, three to four time constants were sufficient for a satisfactory global fit. Nevertheless, it should be kept in mind that a sum of exponential functions is only a rough approximation of the underlying molecular processes.

entire data set was additionally analyzed by singular value decomposition (SVD) and a qualitative visualization technique. Both methods confirm the reaction model derived from the global fitting routine.

The *cis* → *trans* reaction

As discussed above, transient spectra of the various AMPB samples behave in a very similar way. Only a more detailed inspection reveals specific sample characteristics: The difference spectra at $t_D = 200$ fs allow obtaining information on the excited electronic state reached by the excitation process after the early part of the relaxation process (see Fig. 5). At 200-fs induced absorption (excited state absorption) into two broad bands is observed: at short wavelengths the induced absorption peaks at or below 350 nm, close to the peak of the *trans* absorption band. A broad absorption extends from 470 nm to the red part of the spectrum with its maximum at 580 nm. It is only in the range of the *cis* $n\pi^*$ transition that reduced absorption (bleaching of the *cis* $n\pi^*$ band) is found.

On the subpicosecond timescale there is a rapid decrease of the absorption in the red part of the spectrum ($\lambda_{pr} > 550$ nm) and in the shoulder of the 350-nm band between 380 nm and 420 nm. Close to the peak of the 350-nm band an absorption increase is observed. These spectral transients occur on the 200-fs timescale; the fitting procedure results in time constants of 190 fs (c-AMPB) and 280 fs (bc-AMPB; see Table 2).

The spectral signatures of the early absorption changes, especially the strong absorption increase around 350 nm in the *trans* $\pi\pi^*$ band, indicate that the AMPB molecules undergo a very rapid isomerization to the *trans* form of the chromophore. The *trans* absorption band is built up to a considerable extent (40–70% of its final value) on the subpicosecond timescale for all AMPB samples. The early transient spectra (Fig. 5) and the spectral signature of the ~200-fs kinetic components (Fig. 6) of the decay associated spectra indicate that the excited state absorption spectra have two strong bands at 400 nm and around 580 nm. The negative amplitudes of the decay associated spectra below 380 nm and between 430 nm and 500 nm point to the rapid reformation of the *trans* $\pi\pi^*$ and $n\pi^*$ absorption bands. All the signatures are indicative for a very rapid decay of the excited electronic state and a rapid formation of the ground state photoproduct.

Subsequent absorption changes occur on the picosecond timescale. The different samples exhibit similar time constants of ~2 ps and ~10 ps but show certain systematic deviations in the decay associated spectra. There is always increased absorption around the center of the *trans* $\pi\pi^*$ band (at 350 nm) and a weak absorption decrease in its red wing (around 380 nm). The spectral signatures in this range indicate that the 2-ps and the 10-ps processes are related to the cooling of the vibrationally hot chromophore, i.e., the $\pi\pi^*$ band exhibits the well known decrease of the red wing absorption band and a decreasing band width, typical for the cooling process of a hot chromophore. Similar picosecond time constants and spectral signatures have been observed for the cooling of a number of dye molecules including azobenzene (Hamm et al., 1997; Nägele et al., 1997).

In the same time range, different spectral features are found for free AMPB and AMPB peptides, respectively: the free chromophore AMPB displays similar decay associated spectra for the 2-ps and the ~10-ps components. Such a behavior is expected for a cooling process (Hamm et al., 1997; Nägele et al., 1997; Spörlein et al., 2002). Interestingly, the spectra of the AMPB peptides behave in a different way: whereas the 2-ps component peaks around 530 nm, the 10-ps component is shifted to the blue with a maximum around 500 nm.

The ~10-ps component is the slowest observed in the AMPB chromophore. For the AMPB peptides there are additional slower absorption changes with relatively weak amplitudes.

Linear AMPB shows a slow absorption decrease on the timescale of 60 ps throughout the whole spectral range. There is a pronounced rise of this absorption change in the red wing of the *trans* band with a peak at 370 nm. The steep decrease to short wavelengths indicates a small blue shift of the *trans* band during the 60-ps process. This observation points to a slow relaxation on the strain of the AMPB chromophore upon motion of the linear peptide chain (Spörlein et al., 2002). The inspection of the transient IR data (Bredenbeck et al., 2003) of linear AMPB reveals IR absorption changes in the same time domain. The absorption change persistent at ~1 ns is similar to the cw-difference spectrum indicating that the chromophore has acquired its final structure.

The monocyclic c-AMPB peptide shows a slow kinetic component in the 180-ps range. Its spectral signature is similar to the one of l-AMPB, however with a stronger growth of the *trans* band. Apparently the monocyclic geom-

etry leads to stronger interactions between peptide and chromophore extending also to longer times.

The bicyclic peptide bc-AMPB displays absorption transients extending to even longer times. One can model these kinetic components with two time constants of ~100 ps and ~1 ns. Both kinetics reproduce qualitatively the spectral signature found in c-AMPB. There are different positions of the peak absorption change in the red wing of the newly formed *trans* band. This clearly points to relaxational processes spanning a wide timescale, reducing stepwise the strain on the chromophore molecule. It should be noted that the results of the time-resolved infrared experiment agree well with the observation in the visible spectral range (Bredenbeck et al., 2003). They support the given interpretation of the slower process as a structural rearrangement of the peptide moiety. The infrared experiments show a fast and strong absorption change in the amide I band due to structural changes in the time range of 5–20 ps that should be compared with the 5.3-ps component. For longer delay times the IR experiment reveals structure related absorption transients also seen in the visible experiments.

The *trans* → *cis* reaction

Immediately after light absorption at 480 nm, the AMPB chromophore shows a very broad absorption spectrum (Fig. 5 *b*). For $\lambda > 380$ nm, there is pronounced excited state absorption that seems to be composed of two bands, one centered at 430 nm and one at 550 nm. In the 350-nm range, there is a strong signal reduction, due to the bleaching of the *trans* $\pi\pi^*$ ground state absorption. As a striking difference to the *cis* → *trans* reaction, there is a pronounced absorption increase and not a bleach in the 400-nm range. It is interesting to note that qualitatively the same absorption changes are observed also in the AMPB peptides.

On the subpicosecond timescale, there are only small additional absorption changes for AMPB, l-AMPB, and c-AMPB with time constants in the 500-fs range. Only the bicyclic peptide bc-AMPB shows a more pronounced and faster (300 fs) subpicosecond component. The similarity of the transient spectra at 200 fs and 2 ps indicates that a significant part of the molecules remains in the excited electronic state even at 2 ps. This finding is supported by the observation that the bleach of the 350-nm band does not recover during the first 2 ps.

Subsequent absorption changes on the <20-ps timescale contain components with ~1.5 ps and ~9 ps, with stronger absorption transients of the slower component. In both processes the strong excited state absorption band at 430 nm and the bleach of the *trans* band (350 nm) recover to a large extent. The spectral signatures indicate that the internal conversion to the ground state finally occurs with the ~9-ps kinetic process. Since this reaction is on the same timescale as the vibrational cooling, the latter process may contribute to the transient spectrum, but does not appear as a separate kinetic component.

At later delay times one finds only weak absorption transients. For l-AMPB and c-AMPB, these weak kinetic components are in the order of ~100 ps. Since their amplitudes are close the experimental noise, they should not be discussed here in more detail.

DISCUSSION

Cyclic model peptides with built-in light switches act as model systems, where conformational peptide dynamics can be synchronously initiated and observed with high temporal resolution. After the first real time observation of elementary events in an APB peptide for the *cis* → *trans* isomerization (Spörlein et al., 2002), this work is focused on the following questions:

- Does the modification of the molecular design with a more flexible switching molecule affect the viability of the experimental approach?
- How does the increased flexibility of the cyclic azopeptide construct caused by the introduction of the methylene spacer between chromophore and peptide moiety change photopyhsical properties like electronic transition energies, reaction rate or quantum yield?
- How (fast) is the geometrical change of the chromophore transmitted to the peptide chain?
- Is the dynamics of the moving backbone detectable via the absorption transients of the chromophore in the visible spectral range?

For a detailed understanding of the AMPB-peptide dynamics, one has to take into account the experimental observations that the modification of azobenzene to the AMPB chromophore has a profound effect on its electronic (Table 1 and Fig. 2) and dynamic (Table 2 and Figs. 3–5) properties. The dynamic effects will be discussed here along the hierarchal sequence of investigated systems: the ultrafast photoresponse of the chromophore AMPB defines the trigger signal with an intramolecular geometrical change driven by the isomerization. The linear peptide l-AMPB has virtually the same molecular mass than the cyclic peptides and allows the study of inertia effects on the primary photoreaction, though without any conformational restrictions. The identical absorption properties of the three peptide systems (Fig. 2) allow their direct spectroscopic comparison. The cyclic c-AMPB and bicyclic bc-AMPB molecules finally allow the discussion of peptide motion under the action of different constraints.

The AMPB chromophore

The ultrafast photodynamics of azobenzene were investigated in numerous experimental and theoretical studies (Lednev et al., 1996; Hamm et al., 1997; Nägele et al., 1997;

Lednev et al., 1998; Fujino et al., 2002). Recently, the excited state surface was probed by time-resolved absorption and fluorescence techniques (Lu et al., 2002; Satzger et al., 2003), elucidating the differences for the two isomerization directions in more detail. However, no experimental data on AMPB have been reported so far. Compared to APB, with a strong overlap of $n\pi^*$ and $\pi\pi^*$ bands (see Table 1 and Wachtveitl et al., 1997; Spörlein et al., 2002), the spectrum of AMPB is more azobenzene-like. The $n\pi^*$ and $\pi\pi^*$ bands are well separated and allow a defined $S_0 \rightarrow S_1$ photoexcitation.

In the *trans* → *cis* reaction, the dynamic behavior for early delay times is described by three kinetic components with similar signal height in the amplitude spectrum (Fig. 6 *b*). The spectral signature of the 470-fs component leads to the assumption that it represents a movement out of the Franck-Condon region. This is supported by recent fluorescence studies on azobenzene (Satzger et al., 2003). The fact that the two kinetic components (1.6 ps and 7.9 ps) exhibit a similar spectral signature with distinct excited state characteristics for $\lambda_{pr} > 530$ nm (Fig. 6 *b*) leads to the conclusion that the S_1 potential energy surface is left in a multiphasic way on the picosecond time range. The positive signal for $\lambda_{pr} > 400$ nm indicates the excited state decay, the negative signal in the region of the $\pi\pi^*$ band ($\lambda_{pr} > 400$ nm), demonstrates the repopulation of the *trans* ground state. The bleach of the 350-nm *trans* absorption band observed at late times is a direct indication for the formation of the photoproduct (*cis* AMPB).

The *cis* → *trans* photoreaction (Figs. 5 *a* and 6 *a*) is considerably faster than the *trans* → *cis* reaction. Three kinetic components (250 fs, 2.9 ps, and 12 ps) result from the analysis of the transient absorption data. The fastest 250-fs component has the largest amplitude and shows the spectral signatures expected for a S_1 decay. Interestingly, for the two slower and weaker components the decay associated spectra are different. This finding indicates that the slower decaying states are not identical with the original Franck-Condon state. They may be reached by motions on the S_1 surface. The relative amplitude of the newly formed 350-nm band indicates that ~40–50% of the molecules react within the first 250 fs to the *cis* photoproduct.

The quantum yield of the isomerization can be estimated by calculating both the percentage of photoexcited molecules per pump pulse within the irradiated sample volume (*trans* → *cis*: 2.5%; *cis* → *trans*: 2.8%) and the difference spectrum $D(\lambda) = A_{trans(cis)}(\lambda) - A_{cis(trans)}(\lambda)$ scaled for the respective sample concentrations in the femtosecond experiment. The ratio of the signal amplitude at $t_D = 1$ ns and the signal size in the difference spectrum allows the estimating of how many of the photoexcited molecules isomerize. The quantum yields obtained from that procedure are ≈20% for the *trans* → *cis* and ≈70% for the *cis* → *trans* isomerization.

It can be concluded that AMPB acts as an efficient, ultrafast switch for the *cis* to *trans* reaction, although switching efficiency as well as switching speed are less optimal for the *trans* to *cis* reaction. In general, the isomerization occurs somewhat slower and exhibits a more disperse temporal behavior than for azobenzene.

Common features of azobenzene peptides

For both isomerization directions the kinetic component with the fastest time constant is weaker in AMPB peptides than in the free chromophore AMPB. This leads to an overall slower reaction dynamics with a pronounced multiexponential character. This behavior is expected since 1), the inertia of the peptide chain should slow down the conformational transition and 2), the different initial conformations of the backbone of the peptide should lead to distributed kinetics. Apparently the reaction paths from the Franck-Condon region toward the minimum of the S_1 potential energy surface are modified by various local minima acting as kinetic traps. Furthermore, 3), the feedback of the peptide chain and its subsequent rearrangement on the chromophore leads to slow absorption kinetics not present in the free AMPB chromophore.

The l-AMPB peptide

In the case of l-AMPB small absorption changes on the timescale of 20–100 ps are observed. These changes reflect the response of the peptide part on the changed AMPB structure. Photoizomerization of the chromophore forces parts of the peptide away from their initial positions. The reaction toward the new equilibrium relaxes the strain on AMPB and is therefore visible via the absorption dynamics. The weak differences in the stationary *cis* → *trans* infrared difference spectra in the amide I range indicate that the structure of the peptide moiety is slightly different for the two states of the chromophore. Since the peptide part of the linear l-AMPB molecule is not restricted by cyclization, the observed persistent changes of the amide I band must be due to direct contact to the AMPB molecule and is apparently related to amino acids close to the chromophore. Similar conformational changes have been observed in linear flexible proline containing azopeptides (Rudolph-Böhner et al., 1997).

The cyclic AMPB peptides

Peptide backbone cyclization drastically restricts the number of accessible conformational states and leads to distinct structures of the peptide part for the two isomers of the chromophore. The direct comparison to l-AMPB allows to single out the dynamic consequences for these confined systems and to observe in real time the structural transitions. Based on the results derived from NMR structural analysis (Renner et al., 2000b), the largest structural changes are expected for the *cis* → *trans* isomerization of bc-AMPB, since the restrictions of the conformational space for *trans*

bc-AMPB lead to a well-defined structure (smallest root mean-square deviation values).

The trans → cis reaction

A comparison of the peptide samples demonstrates a qualitative similarity between c-AMPB, bc-AMPB, and l-AMPB both in the transient and in the amplitude spectra for several parts of the spectrum. A direct comparison of individual transients or transient spectra (Fig. 5) still shows an almost identical decay for l-AMPB and c-AMPB, but an accelerated decay for bc-AMPB. Due to the additional conformational restraints in the disulfide-bridged bc-AMPB, a guided, reactive motion out of the Franck-Condon region may be favored. A similar accelerated initial photoreaction was also observed for c-APB peptides (Spörlein et al., 2002). On the timescale of a few picoseconds, the initial strain is released and the cyclization of the peptide has only little influence on the observed dynamics. The amplitude spectra of the 1.6-ps and the 10 ps time constants of bc-AMPB indicate that the transition from the excited state to the initial *trans* ground state occurs on this timescale. The total amount of photoproduct formation can be analyzed for short probing wavelengths ($\lambda_{pr} < 400$ nm). The amplitude of the long time offset in the region of the $\pi\pi^*$ band indicates that the quantum yield for the cyclized peptides c-AMPB and bc-AMPB is significantly higher than for the linear peptide l-AMPB. It can therefore be concluded that cyclization favors the productive isomerization pathway, whereas further conformational restriction (c-AMPB → bc-AMPB) accelerates the initial reaction but leaves the quantum yield unaffected.

The cis → trans reaction

At early delay times the onset of a *trans*-isomer absorption and a decrease of the excited state absorption around 400 nm due to rapid product formation is observed. This reaction occurs with the fastest time constant determined in the fitting procedure and contributes strongly in both cyclic molecules. However, the fraction of fast reacting molecules is reduced in bc-AMPB in favor of the slower components (Fig. 6 *g*) as compared to c-AMPB. Obviously bc-AMPB starts preferably from conformations that do not support ultrafast isomerization dynamics. The intermediate time constants exhibit an amplitude spectrum that emphasizes that this reaction is a $S_1 \rightarrow S_0$ transition forming an intermediate *trans*-like state. The later reaction dynamics show that this state reached within a few picoseconds has not yet relaxed to the final ground state structure The spectrum of the 180-ps time constant of c-AMPB (Fig. 6 *e*) as well as the ones of the 100-ps and 1-ns component in bc-AMPB (Fig. 6 *g*) point to a transition of the chromophore from a distorted to a more planar geometry as the peptide backbone gradually relaxes. The spectral signature of these components is indicative for a transition on the ground state energy surface representing a band shift of the photoproduct absorption upon relaxation of the strain on the chromophore (see Fig. 7). The shape of the 100-ps amplitude spectrum in the 350–400-nm range is very well reproduced by a model curve assuming a reduced red shift of the *trans* $\pi\pi^*$ band from 15 nm to 5 nm compared to the relaxed *trans* conformation. This transition is schematically sketched in Fig. 7. Thus the late ($\tau \approx 1$ ns) spectral changes are assigned to further conformational relaxation of the molecule: the reduced amplitude for long probing wavelengths and the $\pi\pi^*$ band signal meet the expectations for the approach to the relaxed *trans* ground state.

The sequence of events can therefore be summarized as follows: after photoexcitation the return to the S_0 energy surface occurs multiexponentially and is completed within a few picoseconds. These events are connected with the isomerization of the chromophore. The subsequent processes occur on the ground state potential energy surface: the isomerized molecules act on the peptide part and induce further structural changes. During this process the strain upon the chromophore decreases with the alignment of the peptide units allowing a relaxation toward the minimum of the S_0 potential energy surface. This relaxation is not finished within a few picoseconds. Energetically elevated intermediate states are populated that allow the chromophore to adopt *trans*-like, yet somewhat twisted, conformations. The slow absorption transients indicate that the main conformational changes of the cyclic peptides are completed on the fast timescale of 10 ps–1 ns. The subsequent structural fine-tuning of the peptide is small and does not show up in the visible spectrum. Therefore the question of slower and more subtle rearrangements of the peptide backbone has to be addressed with time-resolved structure sensitive techniques such as pico- and nanosecond infrared experiments

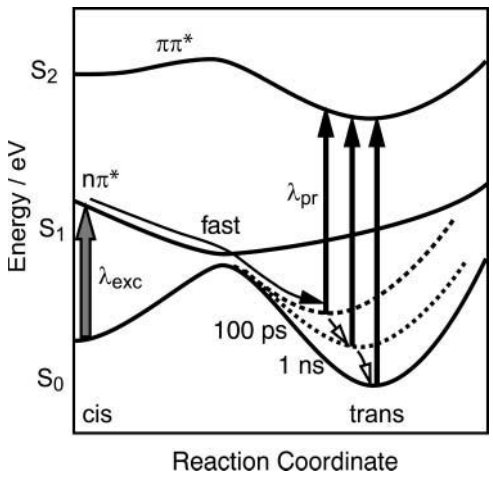

FIGURE 7 Simplified picture of a one-dimensional potential energy surface describing the *cis* → *trans* isomerization reaction pathway of cyclic azopeptides (modified, after Monti et al., 1982).

(Bredenbeck et al., 2003). It should be pointed out that our results not only address the early events in peptide folding, but that the fast dynamics observed in this system with highly restricted conformational space should also have important implications for rearrangements of folded structures.

CONCLUSIONS

The photoresponse of small peptides with the built-in light switch AMPB containing a methylene group as flexible spacer was investigated in the visible spectral range with subpicosecond time resolution. The spectroscopic data allow assigning timescales to the individual reaction steps that are isomerization, vibrational cooling, and alignment of the peptide part. The results demonstrate that for such systems with a sufficiently strong driving force a significant part of the nonequilibrium conformational dynamics occurs on the picosecond timescale, i.e., much faster than the intrachain diffusion rates determined for peptides of comparable size (Bieri et al., 1999). The kinetic contributions in the picosecond to nanosecond range reveal the complex nature of the early reaction steps even for small peptides. Nevertheless, the systematic evaluation of isomerization rates and quantum yields for the various model systems may allow deducing first simple rules for the understanding and prediction of early processes in peptide folding.

Funding for this study has been provided by the Sonderforschungsbereiche 533 and 472 of the Deutsche Forschungsgemeinschaft.

REFERENCES

Ballew, R. M., J. Sabelko, and M. Gruebele. 1996. Observation of distinct nanosecond and microsecond protein folding events. *Nat. Struct. Biol.* 3:923–926.

Behrendt, R., C. Renner, M. Schenk, F. Q. Wang, J. Wachtveitl, D. Oesterhelt, and L. Moroder. 1999a. Photomodulation of the conformation of cyclic peptides with azobenzene moieties in the peptide backbone. *Angew. Chem. Int. Ed.* 38:2771–2774.

Behrendt, R., M. Schenk, H.-J. Musiol, and L. Moroder. 1999b. Photomodulation of conformational states. Synthesis of cyclic peptides with backbone-azobenzene moieties. *J. Pept. Sci.* 5:519–529.

Bieri, O., and T. Kiefhaber. 1999. Elementary steps in protein folding. *Biol. Chem.* 380:923–929.

Bieri, O., J. Wirz, B. Hellrung, M. Schutkowski, M. Drewello, and T. Kiefhaber. 1999. The speed limit for protein folding measured by triplet-triplet energy transfer. *Proc. Natl. Acad. Sci. USA.* 96:9597–9601.

Bredenbeck, J., J. Helbing, A. Sieg, T. Schrader, W. Zinth, C. Renner, R. Behrendt, L. Moroder, J. Wachtveitl, and P. Hamm. 2003. Picosecond conformational transition and equilibration of a cyclic peptide. *Proc. Natl. Acad. Sci. USA.* 100:6452–6457.

Cattani-Scholz, A., C. Renner, C. Cabrele, R. Behrendt, D. Oesterhelt, and L. Moroder. 2001. Photoresponsive cyclic bis(cysteinyl)peptides as catalysts of oxidative protein folding. *Angew. Chem. Int. Ed.* 41: 289–292.

Daura, X., W. F. van Gunsteren, and A. E. Mark. 1999. Folding-unfolding thermodynamics of a beta-heptapeptide from equilibrium simulations. *Proteins.* 34:269–280.

Dill, K. A., and H. S. Chan. 1997. From levinthal to pathways to funnels. *Nat. Struct. Biol.* 4:10–19.

Duan, Y., and P. A. Kollman. 1998. Pathways to a protein folding intermediate observed in a 1-microsecond simulation in aqueous solution. *Science.* 282:740–744.

Frauenfelder, H., S. G. Sligar, and P. G. Wolynes. 1991. The energy landscapes and motions of proteins. *Science.* 254:1598–1603.

Fujino, T., S. Y. Arzhantsev, and T. Tahara. 2002. Femtosecond/picosecond time-resolved spectroscopy of trans-azobenzene: isomerization mechanism following $S_2(\pi\pi^*) \leftarrow S_0$ photoexcitation. *Bull. Chem. Soc. Jpn.* 75:1031–1040.

Gilmanshin, R., S. Williams, R. H. Callender, W. H. Woodruff, and R. B. Dyer. 1997. Fast events in protein folding: relaxation dynamics of secondary and tertiary structure in native apomyoglobin. *Proc. Natl. Acad. Sci. USA.* 94:3709–3713.

Hamm, P., S. M. Ohline, and W. Zinth. 1997. Vibrational cooling after ultrafast photoisomerization of azobenzene measured by femtosecond infrared spectroscopy. *J. Chem. Phys.* 106:519–529.

Huang, C. Y., Z. Getahun, Y. J. Zhu, J. W. Klemke, W. F. DeGrado, and F. Gai. 2002a. Helix formation via conformation diffusion search. *Proc. Natl. Acad. Sci. USA.* 99:2788–2793.

Huang, C. Y., S. He, W. F. DeGrado, D. G. McCafferty, and F. Gai. 2002b. Light-induced helix formation. *J. Am. Chem. Soc.* 124:12674–12675.

Huber, R., J. E. Moser, M. Grätzel, and J. Wachtveitl. 2002. Real-time observation of photoinduced adiabatic electron transfer in strongly coupled dye/semiconductor colloidal systems with a 6 fs time constant. *J. Phys. Chem. B.* 106:6494–6499.

Huber, R., H. Satzger, W. Zinth, and J. Wachtveitl. 2001. Noncollinear optical parametric amplifiers with output parameters improved by the application of a white light continuum generated in CaF_2. *Opt. Comm.* 194:443–448.

Krimm, S., and J. Bandekar. 1986. Vibrational spectroscopy and conformation of peptides, polypeptides, and proteins. *Adv. Protein Chem.* 38:181–364.

Lednev, I. K., T. Ye, R. E. Hester, and J. N. Moore. 1996. Femtosecond time-resolved uv-visible absorption spectroscopy of *trans*-azobenzene in solution. *J. Phys. Chem.* 100:13338–13341.

Lednev, I. K., T. Ye, P. Matousek, M. Towrie, P. Foggi, F. V. R. Neuwahl, S. Umapathy, R. E. Hester, and J. N. Moore. 1998. Femtosecond time-resolved uv-visible absorption spectroscopy of *trans*-azobenzene: dependence on excitation wavelength. *Chem. Phys. Lett.* 290:68–74.

Lu, Y. C., C. W. Chang, and E. W. G. Diau. 2002. Femtosecond fluorescence dynamics of trans-azobenzene in hexane on excitation to the s1(n,π^*) state. *J. Chin. Chem. Soc.-TAIP.* 49:693–701.

Monti, S., G. Orlandi, and P. Palmieri. 1982. Features of the photochemically active state surfaces of azobenzene. *Chem. Phys.* 71:87–99.

Munoz, V., P. A. Thompson, J. Hofrichter, and W. A. Eaton. 1997. Folding dynamics and mechanism of beta-hairpin formation. *Nature.* 390: 196–199.

Nägele, T., R. Hoche, W. Zinth, and J. Wachtveitl. 1997. Femtosecond photoisomerization of *cis*-azobenzene. *Chem. Phys. Lett.* 272:489–495.

Pollack, L., M. W. Tate, A. C. Finnefrock, C. Kalidas, S. Trotter, N. C. Darnton, L. Lurio, R. H. Austin, C. A. Batt, S. M. Gruner, and S. G. Mochrie. 2001. Time resolved collapse of a folding protein observed with small angle x-ray scattering. *Phys. Rev. Lett.* 86:4962–4965.

Rau, H. 1990. Azo compounds. *In* Studies in Organic Chemistry, Photochroism, Molecules and Systems. H. Dürr and H. Bouas-Laurent, editors. Elsevier, Amsterdam, The Netherlands. 165–192.

Renner, C., R. Behrendt, N. Heim, and L. Moroder. 2002. Photomodulation of conformational states. III. Water-soluble bis-cysteinyl-peptides with (4-aminomethyl) phenylazobenzoic acid as backbone constituent. *Biopolymers.* 63:382–393.

Renner, C., R. Behrendt, S. Spörlein, J. Wachtveitl, and L. Moroder. 2000a. Photomodulation of conformational states. I. Mono- and bicyclic peptides with (4-amino)phenylazobenzoic acid as backbone constituent. *Biopolymers.* 54:489–500.

Renner, C., J. Cramer, R. Behrendt, and L. Moroder. 2000b. Photomodulation of conformational states. II. Mono- and bicyclic peptides with (4-aminomethyl)phenylazobenzoic acid as backbone constituent. *Biopolymers.* 54:501–514.

Rudolph-Böhner, S., M. Krüger, D. Oesterhelt, L. Moroder, T. Nägele, and J. Wachtveitl. 1997. Photomodulation of conformational states of p-phenylazobenzyloxycarbonyl-l-proline and related peptides. *J. Photochem. Photobiol. A. Chem.* 105:235–248.

Satzger, H., S. Spörlein, C. Root, J. Wachtveitl, W. Zinth, and P. Gilch. 2003. Fluorescence spectra of *trans*- and *cis*-azobenzene - emission from the Franck-Condon state. *Chem. Phys. Lett.* 372:216–223.

Seel, M., E. Wildermuth, and W. Zinth. 1997. A multichannel detection system for application in ultrafast spectroscopy. *Meas. Sci. Technol.* 1997:449–452.

Spörlein, S., H. Carstens, H. Satzger, C. Renner, R. Behrendt, L. Moroder, P. Tavan, W. Zinth, and J. Wachtveitl. 2002. Ultrafast spectroscopy reveals subnanosecond peptide conformational dynamics and validates molecular dynamics simulation. *Proc. Natl. Acad. Sci. USA.* 99:7998–8002.

Thompson, P. A., V. Munoz, G. S. Jas, E. R. Henry, W. A. Eaton, and J. Hofrichter. 2000. The helix-coil kinetics of a heteropeptide. *J. Phys. Chem. B.* 104:378–389.

Torii, H., and M. Tasumi. 1992. Model-calculations on the amide-i infrared bands of globular- proteins. *J. Chem. Phys.* 96:3379–3387.

Torii, H., and M. Tasumi. 1998. Ab initio molecular orbital study of the amide I vibrational interactions between the peptide groups in di- and tripeptides and considerations on the conformation of the extended helix. *J. Raman Spectrosc.* 29:81–86.

Ulysse, L., and J. Chmielewski. 1994. The synthesis of a light-switchable amino-acid for inclusion into conformationally mobile peptides. *Bioorg. Med. Chem. Lett.* 4:2145–2146.

Ulysse, L., J. Cubillos, and J. Chmielewski. 1995. Photoregulation of cyclic peptide conformation. *J. Am. Chem. Soc.* 117:8466–8467.

Volk, M., Y. Kholodenko, H. S. M. Lu, E. A. Gooding, W. F. DeGrado, and R. M. Hochstrasser. 1997. Peptide conformational dynamics and vibrational stark effects following photoinitiated disulfide cleavage. *J. Phys. Chem. B.* 101:8607–8616.

Wachtveitl, J., T. Nägele, B. Puell, W. Zinth, M. Krüger, S. Rudolph-Böhner, D. Oesterhelt, and L. Moroder. 1997. Ultrafast photoisomerization of azobenzene compounds. *J. Photochem. Photobiol. A. Chem.* 105:283–288.

Werner, J. H., R. B. Dyer, R. M. Fesinmeyer, and N. H. Andersen. 2002. Dynamics of the primary processes of protein folding: helix nucleation. *J. Phys. Chem. B.* 106:487–494.

Wilhelm, T., J. Piel, and E. Riedle. 1997. Sub-20-fs pulses tunable across the visible from a blue-pumped single-pass noncollinear parametric converter. *Opt. Lett.* 22:1494–1496.

Williams, S., T. P. Causgrove, R. Gilmanshin, K. S. Fang, R. H. Callender, W. H. Woodruff, and R. B. Dyer. 1996. Fast events in protein folding: helix melting and formation in a small peptide. *Biochemistry.* 35: 691–697.

Zhou, Y. Q., and M. Karplus. 1999. Interpreting the folding kinetics of helical proteins. *Nature.* 401:400–403.